BMPR-II deficiency elicits pro-proliferative and anti-apoptotic responses through the activation of TGFβ-TAK1-MAPK pathways in PAH

Md Talat Nasim [1,2]*; Takeshi Ogo [1]; Hasnin M. Chowdhury [1]; Lan Zhao [3]; Chien-nien Chen[3] ; Christopher Rhodes [3] ; and Richard C. Trembath [1,2]

[1] Department of Medical and Molecular Genetics, King's College London, London, United Kingdom , [2] National Institute for Health Research (NIHR), Biomedical Research Centre, Guy's and St. Thomas' NHS Foundation Trust and King's College London, London, United Kingdom, [3]Pharmacology and Therapeutics, Experimental Medicine, Hammersmith Hospital, Imperial College London, London, United Kingdom.

Correspondence can be addressed to

*Dr. M. T. Nasim

King's College London

Dept. of Medical and Molecular Genetics

Tower Wing, Guy's Hospital

London SE1 9RT, United Kingdom

Tel: +44 (0) 20-7188 -9505, Fax: +44 (0) 20-7188 -2885

Email: talat.nasim@ kcl.ac.uk

Abstract

Pulmonary arterial hypertension (PAH) is a cardiovascular disorder associated with enhanced proliferation and suppressed apoptosis of pulmonary arterial smooth muscle cells (PASMCs). Heterozygous mutations in the type II receptor for bone morphogenetic protein (*BMPR2*) underlie the majority of the inherited and familial forms of PAH. The transforming growth factor β (TGFβ) pathway is activated in both human and experimental models of PAH. However, how these factors exert pro-proliferative and anti-apoptotic responses in PAH remains unclear. Using mouse primary PASMCs derived from knock-in (KI) mice, we demonstrated that BMPR-II dysfunction promotes the activation of SMAD-independent MAPK pathways via TGFβ-associated kinase 1 (TAK1), resulting in a pro-proliferative and anti-apoptotic response. Inhibition of the TAK1-MAPK axis rescues abnormal proliferation and apoptosis in these cells. In both hypoxia and monocrotaline-induced PAH rat models, which display reduced levels of *bmpr2* transcripts, this study further indicates that the TGFβ-MAPK axis is activated in lungs following elevation of both expression and phosphorylation of TAK1 protein. In *ex-vivo* cell based assays, TAK1 inhibits BMP-responsive reporter activity and interacts with BMPR-II receptor. In the presence of pathogenic *BMPR2* mutations observed in PAH patients, this interaction is greatly reduced. Taken together, these data suggest dysfunctional BMPR-II responsiveness intensifies TGFβ-TAK1-MAPK signaling and thus alters the ratio of apoptosis to proliferation. This axis may be a potential therapeutic target in PAH.

Key words- Pulmonary arterial hypertension, BMPR-II receptor, TGFβ signaling, TAK1 and MAPK.

Introduction

Pulmonary arterial hypertension (PAH) is a severe vascular disorder characterized by narrowing and obliteration of the small pulmonary arteries due to abnormal proliferation of endothelial and smooth muscle cells. Pulmonary vasoconstriction and vascular remodeling leads to elevation of pulmonary artery pressure and, in the absence of an effective therapy, eventual right-heart failure and death. Heterozygous nonsense mutations in the gene encoding the type II receptor for bone morphogenetic protein (BMPR-II), a member of the TGFβ receptor family, underlie the majority of inherited and familial forms of PAH (1). Levels of *BMPR2* transcripts and proteins are reduced in the lungs in both familial and sporadic PAH patients with and without *BMPR2* mutation (2, 3).

BMPR-II–mediated signaling regulates vascular cell survival and proliferation, but the underlying mechanisms are complicated. BMP2 and 7 inhibit the proliferation of human and rat smooth muscle cells (4, 5) via the small mothers against decapentaplegia (SMAD) pathway (6). In PASMCs isolated from PAH subjects (PAH-PASMCs), the anti-proliferative effect of BMPs (2, 4 and 7) is greatly reduced (7). Furthermore, BMP-promoted apoptosis in PAH-PASMCs with reduced BMPR-II protein levels is attenuated (8). Similarly, TGFβ signaling accelerates proliferation in PAH-PASMCs, whereas it inhibits proliferation in normal PASMCs (7). Elevated TGFβ activity has been reported in rat monocrotaline and hypoxia models of PAH, and inhibitors of the TGFβ type I receptor (ALK5) prevent the development and progression of disease in these models (9, 10). These findings suggest the involvement of an activated TGFβ pathway in PAH.

TGFβ superfamily ligands signal through both SMAD-dependent and SMAD-independent pathways. SMAD signaling occurs via either SMAD2/3 (TGFβ) or SMAD1/5/8 (BMP), which translocate to the nucleus with the common SMAD (SMAD4) to directly regulate target gene transcription (11). BMPs and TGFβs have both been reported to activate SMAD-independent mitogen activated protein kinase (MAPK) signaling pathways including ERK, JNK and p38MAPK (6). Phosphorylation of p38MAPK and ERK1/2 is increased in PAH-PASMCs and experimental models of PAH (12-16). Inhibition of MAPK decreases the excessive proliferation of PAH-PASMCs (3) and prevents progression of the disease in model systems, suggesting that SMAD-independent pathways play a key role in disease pathogenesis. However, the molecular mechanism by which TGFβ-induced SMAD-independent pathways might be activated consequent to impaired BMPR-II signaling remain unknown.

TGFβ-associated kinase 1 (TAK1), a member of the MAPK kinase kinase (MAPKKK) family, has been shown to be an important regulator of SMAD-independent MAPK kinase activation in both the TGFβ and BMP signaling pathways. TAK1 modulates a number of processes ranging from innate immune responses to patterning and differentiation via several signaling molecules, including p38MAPK, ERK, JNK, NFkappaB and TCFbeta-catenin. TAK1 also facilitates cross talk between signaling pathways. Such links via TAK1 have been established between TGFβ and oncogenic R-Ras in the promotion of tumorigenesis (17) and between BMP and PI3K/Akt in cardiac cell growth and survival in the postnatal heart (18). We hypothesized that the activation of SMAD-independent MAPK pathways in PAH consequent to impaired BMPR-II signaling is mediated via TAK1.

In this report, we demonstrated that in mouse PASMCs, BMPR-II dysfunction promotes the activation of SMAD-independent MAPK pathways via TAK1 resulting in a pro-proliferative

and anti-apoptotic response. Inhibition of the TAK1-MAPK axis rescues abnormal proliferation and apoptosis in these cells. We provide *in vivo* support of the *in vitro* findings in two independent PAH rat models, in which the TGFβ-MAPK axis is activated following elevation of both the expression and phosphorylation of TAK1 protein. In *ex vivo* cell based assays, TAK1 interacts with BMPR-II receptor and in the presence of pathogenic *BMPR2* mutation this interaction in greatly reduced. TAK1 attenuates BMP signaling by inhibiting the phosphorylation of SMAD1 protein.

Results

BMPR-II haploinsufficiency potentiates TGFβ signaling, exerting a pro-proliferative response in mouse primary PASMCs

The effect of reduced levels of BMPR-II on TGFβ signaling was investigated in mouse primary PASMCs and hypoxia-induced PAH rat lung. The level of plasminogen activator inhibitor (*PAI*-1) transcripts was determined as a measure of TGFβ signaling (9, 10). *PAI*-1 expression was increased in transgenic knock-in (KI) mouse primary PASMCs with a PAH-associated *bmpr*2 nonsense mutation (*bmpr2* $^{R899X\ +/-}$) compared to wild-type PASMCs (*bmpr2*$^{+/+}$) (Figure 1A). Reduced levels of transcripts for *bmpr2* and the inhibitor of DNA binding (*Id*1), a known BMP target, were seen in mutant cells (see Supplementary Figure 1A-B). Increased *PAI*-1 expression was also observed in hypoxic rat lung tissue compared to normoxic control tissue (Figure 1B) with a significant decrease in *bmpr2* transcripts (Supplementary Figure 1C). Taken together these data suggest a link between dysfunctional BMPR-II-mediated signaling and activation of the TGFβ pathway.

Proliferation was increased in mutant PASMCs compared to wild-type cells (Figure 1C). As in human control and PAH-PASMCs (7), TGFβ1 stimulation inhibited proliferation in wild-

type mouse PASMCs but promoted proliferation in mutant cells (Figure 1D). Inhibition of p38MAPK signaling by SB203580 reduced the TGFβ1-stimulated cell proliferation in mutant cells. In these cells, the basal level of p38MAPK phosphorylation is higher, and TGFβ1 further activates p38MAPK phosphorylation (Figure 1E-F). Taken together, these data suggest that the pro-proliferative response of mutant cells to TGFβ1 is mediated via the SMAD-independent p38MAPK pathway.

Small molecule inhibitors of the TGFβ -MAPK axis rescue abnormal cell proliferation and apoptosis in mouse PASMCs

We examined the role of TGFβ-mediated SMAD-independent MAPK axis on pro-proliferative activity of *bmpr2* $^{R899X\ +/-}$ PASMCs by chemical agents that selectively inhibit TGFβ and p38MAPK pathways. For inhibition of TGFβ pathway, we employed SD208 which is a known inhibitor of ALK5, a TGFβ type I receptor whilst SB203580 was used to inhibit p38MAPK pathway. ALK5 and p38MAPK inhibitors inhibited proliferation in mutant cells in both the absence (Figure 2A) and presence of TGFβ1 stimulation (Figure 2B), while inhibition of p38MAPK had no discernible effect on wild-type cells. We further investigated whether TAK1, a known activator of p38MPK pathway is involved in exerting the pro-proliferative activity in mutant cells. Treatment with the TAK1 inhibitor (5Z)-7- Oxozeaenol inhibited proliferation in a dose-dependent manner in mutant but not wild-type cells (Figure 2C). Oxozeaenol also reduced TGFβ-stimulated mutant cell proliferation in a dose-dependent manner (Figure 2D).

Next, cysteinyl aspartate protease (caspase) activity was used to measure the effect of p38MAPK, ALK5 and TAK1 inhibitors on apoptosis in mutant cells. The basal activity level of caspases 3 and 7 was attenuated in mutant cells compared to the wild type (Figure 3A), and mutant cells showed a greater response to staurosporine (ST), a known inducer of

caspase-dependent pathways, than wild-type cells (Figure 3B). Treatment with the ALK5 inhibitor SD208 was able to promote apoptosis in both wild-type and mutant cells in the absence (Figure 3C) and presence of TGFβ1 stimulation (Figure 3D), and inhibition of p38MAPK with SB203580 modestly enhanced apoptosis in both wild-type and mutant cells. Oxozeaenol promoted apoptosis in a dose-dependent manner and its pro-apoptotic effects were higher in mutant PASMCs than in the wild type at the two highest doses used (Figure 3E). Consistent with our proliferation data, oxozeaenol induced apoptosis in mutant cells in the presence of TGFβ stimulation in a dose dependent manner (Figure 3F).

In addition to activating p38MAPK, the TAK1 pathway has been shown to activate ERK phosphorylation, which is increased in PAH-PASMCs (3) and experimental PAH animal models (12-16). Similar to the response to oxozeaenol and SB203580 treatment, the ERK inhibitor, U0126, activated caspase 3/7 activity in the absence (Supplementary Figure 2A) and presence of TGFβ stimulation (Supplementary Figure 2B) in mutant cells.

Activation of TAK1-MAPK pathways in hypoxia and monocrotaline-induced PAH rat lungs

Quantitative (Figure 4A) and semi quantitative RT-PCR (Supplementary Figure 3A-B) revealed increased *TAK*1 expression in hypoxic rat lungs compared to normoxic controls. Increased *TAK*1 expression was also observed in PAH-PASMCs harbouring a nonsense *BMPR2* mutation (p.W9X) compared to normal PASMCs (Supplementary Figure 3C). Four isoforms of TAK1 (A-D) have been reported. Western blot analysis of total TAK1 in rat lung tissues identified a long and a short isoform and hence designated here as TAK1-LF and TAK1-SF, respectively (Supplementary Figure 4A). Phosphorylation of neither the long nor the short form was observed in control rat lung tissues (Figure 4B). Interestingly only the TAK1-SF was phosphorylated (Thr184/187) in hypoxic rat lungs after 1 (Figure 4B-C) and 2

weeks (Supplementary Figure 4B-C), but not after 2 days. TAK1-SF was also activated following monocrotaline treatment at 1 week but not at 2 or 4 weeks (Figure 4D-E and Supplementary Figure 4D). The specificity of TAK1-SF was investigated in HEK293 cells. In these cells phosphorylated TAK1-SF but not the TAK1-LF was detected which is consistent with the manufacturer's data (Cell Signaling). The specificity of this protein was tested using oxozeaenol, SMAD1 overexpression and BMP9 stimulation, all of which inhibited phosphorylation, indicating that this protein is TAK1-specific (Supplementary Figure 4E).

The activation of downstream MAPK pathways was investigated in monocrotaline-treated rat lungs. Because treatment with the ERK inhibitor, U0126, induced more pro-apoptotic activity than the p38MAPK inhibitor, SB203580 (compare Supplementary Figs. 2A and 2B with Figs. 3C and 3F, respectively), phosphorylation of ERK1/2 was examined as representative of MAPK phosphorylation. Following three weeks of monocrotaline treatment, phosphorylation of ERK1/2 in the lungs was elevated (Figure 4F-G), while no significant increase was observed after 2 weeks of hypoxic induction (Supplementary Figure 4F).

Signaling crosstalk between SMAD1 and TAK1-mediated pathways

We next investigated the effect of canonical BMP-SMAD signaling on TAK1 activity. Following BMP9 stimulation, a reduced level of endogenous TAK1-SF phosphorylation was observed (Supplementary Figure 5A) in HEK293 cells. In these cells, BMP9 stimulation also inhibited transiently overexpressed TAK1. Reduced level of TAK1 phosphorylation was seen following SMAD1 overexpression (Supplementary Figure 5B). In the presence of an increasing amount of overexpressed TAK1, the SMAD1-mediated inhibition of TAK1 is attenuated (Supplementary Figure 5C).

The effect of TAK1 on BMP signaling was then investigated using a BMP responsive 3GC-lux reporter (19). Overexpression of TAK1 inhibited reporter activity in HEK293 cells (Figure 5A), and transfection of equimolar concentrations of either BMPR-II or type I receptors failed to rescue this TAK1-mediated inhibition (Supplementary Figure 6A). Moreover, overexpression of SMAD1 alone enhanced reporter activity, but SMAD1-mediated reporter activation was markedly reduced in the presence of TAK1 (Supplementary Figure 6B). Transfection of increasing amounts of TAK1 demonstrated that the inhibition of 3GC2-lux reporter activity was dose-dependent (Figure 5B). TAK1-mediated inhibition of BMP signaling was independently confirmed by overexpression of an excess amount of BMPR-II receptor or SMAD1 relative to TAK1 which rescued reporter activity (Supplementary Figure 6C and Figure 5C) and through use of a selective inhibitor of TAK1 (Oxozeaenol) which promoted BMPR-II–mediated reporter activation in a dose-dependent manner (Figure 5D).

TAK1 interacts with BMPR-II receptor

Finally, the link between dysfunctional BMPR-II responsiveness and activation of TGFβ-TAK1-MAPK signaling was investigated. TAK1 interacts with the type II receptor for TGFβ1 namely TGFBRII (20). To investigate the efficiency of a potential interaction between TAK1 and the BMPR-II receptor, fluorescence and enzyme-based mammalian two-hybrid assays were performed (Figure 6A). Co-expression of TAK1 and BMPR-II generated readily detectable dual fluorescence (Figure 6Biii), suggesting an interaction between BMPR-II and TAK1. Overexpression of BMPR-II with ALK3, a known BMPR-II interactor (21), generated greater dual-fluorescence than cells transfected with BMPR-II and TAK1, indicating a weaker interaction between BMPR-II and TAK1 than that observed between BMPR-II and ALK3 (Figure 6Biv). Consistent with the results obtained by fluorescence microscopy, the determination of fluorescence intensity revealed that the efficiency of the

interaction between TAK1 and BMPR-II is weaker than that between BMPR-II and ALK3 (Supplementary Figure 7A-B).

To verify these findings, an enzyme-based (luciferase and β-galactosidase) assay was used to evaluate the interactions between BMPR-II and TAK1 or ALK3 (Figure 6C). Overexpression of BMPR-II with TAK1 generated 200-fold higher luciferase activity compared to reporter alone, further confirming an interaction between these two proteins (Figure 6D). In addition, we were able to replicate the finding that the interaction between BMPR-II and TAK1 is weaker than that of BMPR-II and ALK3 (Figure 6E). Of interest, we noted that the interaction between BMPR-II and TAK1 was significantly reduced by introducing known pathogenic missense *BMPR2* mutations commonly identified in PAH subjects (Figure 6F).

Discussion

The present study provides insight into the mechanism by which dysfunctional BMPR-II and overactive TGFβ –mediated signaling contributes to both pro-proliferative and anti-apoptotic responses leading to the vascular remodelling observed in PAH. In this study we present evidence that suggest BMPR-II deficiency activates TGFβ signaling through the SMAD-independent TAK1-MAPK pathway exerting abnormal proliferation and apoptosis in *bmpr2* $^{R899X\ +/-}$ PASMCs. Inhibition of this TAK1-MAPK axis rescues both abnormal proliferation and apoptosis. Furthermore, we provide *in vivo* support of our *in vitro* findings that TAK1-mediated MAPK pathway is activated in both monocrotaline and hypoxia induced PAH rat models. We demonstrate that TAK1, a kinase which activates MAPK pathways, binds to the BMPR-II receptor. In the presence of PAH-causing *BMPR2* mutations this interaction between BMPR-II and TAK1 is greatly reduced, which may make TAK1 accessible to TGFβ signaling.

This study demonstrated several lines of evidence to suggest that the pro-proliferative response of TGFβ signaling as a consequence of impaired BMPR-II activity is mediated via the TGFβ-TAK1-MAPK axis. We demonstrated that p38MAPK activity and *TAK*1 expression are increased in *bmpr2*-deficient hyperproliferative PASMCs and that the excessive proliferation can be selectively reversed by inhibition of both p38MAPK and TAK1 supporting the finding that inhibition of p38MAPK reverses the vascular dysfunction that is induced by hypoxia (12). We present evidence that the apoptotic resistant phenotype observed in PAH resulting from reduced levels of BMPR-II is modulated via the activation of TAK1-dependent MAPK pathways. Apoptosis is attenuated in mutant PASMCs, an effect that is mitigated by the inhibition of MAPK pathways including TAK1, p38MAPK and ERK. These results imply that *BMPR2* deficiency activates TGFβ-TAK1-MAPK signaling, which may alter the ratio of cell apoptosis to proliferation and thereby mediating pulmonary vascular medial hypertrophy (Figure 7A, 7B).

Both synergistic and antagonistic influences of TAK1 on SMAD-dependent pathways have been reported. TAK1 has been shown to be an essential regulator of BMP signaling and is required for the morphogenesis, growth and maintenance of cartilage (22). In contrast, TAK1 has also been shown to interact with SMAD1-6, which interferes with BMP-induced SMAD signaling in murine mesenchymal progenitor cells (23). In addition, TAK1 inhibits TGFβ-mediated SMAD activity by promotion of p38MAPK signaling in prostate cancer cells (24). In this study, we found that TAK1 inhibits SMAD activity and that the inhibitory effect of TAK1 can be overcome by the promotion of SMAD-mediated signaling, which acts to inhibit TAK1 phosphorylation, indicating a signaling crosstalk between these two pathways (23). These observations support a model in which TAK1 activity is restricted and the protein is retained by the SMADs and/or cellular receptors including BMPR-II and TGFBRII. TAK1 was found to be a BMPR-II–associated protein (18) and, in the presence of pathogenic

missense *BMPR2* mutations (21), the efficiency of the interaction between TAK1 and BMPR-II is markedly reduced. This may impact BMPR-II signaling in two distinct pathways (Figure 7A-B). First, an increase in accessible TAK1 may attenuate SMAD signaling to below threshold level. Second, the increased availability of TAK1 may activate SMAD-independent pathways triggered by the overactive TGFβ signaling as well as by the 'second hit', including inflammation and environmental stress (25) (26).

In an *ex vivo* cell-based model, hypoxia has been shown to increase TAK1 activity (27). Increased expression and phosphorylation of TAK1 in two independent PAH rat models (chronic hypoxia or monocrotaline injection) supports the involvement of activated TAK1-mediated pathway in PAH. Elevated levels of phosphorylated ERK1/2, a downstream target of TAK1, in monocrotaline-induced PH rat lungs further implies the relevance of the TAK1-MAPK axis to PAH. As TAK1 is located at the crossroad of several signaling pathways, the challenge ahead lies in unraveling the context in which it acts together with cellular consequences.

In summary, we have demonstrated that *BMPR2* deficiency exerts pro-proliferative and anti-apoptotic responses through TGFβ-mediated SMAD-independent pathways and that TAK1 plays an essential role in fine tuning both SMAD-dependent and -independent effects in PAH. TAK1-MAPK signaling is involved in cardiac remodelling following myocardial infarction (28) and plays a central role in the maladaptive response to sustained pressure overload (29). Given the therapeutic potential of TAK1 inhibition in pancreatic cancer (30) and myocardial dysfunction caused by chronic pressure overload (29), we propose that the inhibition of the TGFβ-MAPK axis via TAK1 might provide a novel and effective therapeutic intervention in PAH.

Materials and Methods

Further details are provided in Supplementary Materials and Methods.

RNA isolation, cDNA synthesis and reverse Transcriptase PCR (RT-PCR)

Complementary DNA (cDNA) was synthesized using random primers (Roche) and MMLV Reverse Transcriptase (Promega) using RNAs isolated from lung samples as described (31). PCR was carried out using Hi-Fidelity Extensor Master Mix (ABgene).

Cell culture, transient transfection, enzymatic assay and western blots

Cell culture and transfections were carried out as described elsewhere (21) (32). Luciferase and β-galactosidase activities were determined with the Dual-light Reporter Assay (Applied Biosystems) using an ORION-II Plate Luminometer (Berthold) according to manufacturer's protocols. BMP-responsive reporter assay in mammalian cells was performed as previously described (21). Western blots were carried out using anti-phospho specific p38MAPK (Thr180/Thr182), TAK1 (Thr184/187), ERK1/2 (Thr202/Tyr204) and total TAK1 (Cell Signaling) antibodies following manufacturer's protocols. To confirm equal loading the membranes were stripped and re-probed with anti-β-actin antibody (Cell Signaling).

Determination of protein-protein interactions, quantification of proliferation and apoptosis of mouse primary PASMCs

Efficiency of protein-protein interactions between TAK1 and BMPR-II in mammalian cells was determined as previously reported (33). Relative rate of proliferation and apoptosis of mouse PASMC was carried out using CellTiter 96® Aq_{ueous} One Solution Cell Proliferation Assay and Caspase-Glo® 3/7 Assay (Promega) following manufacturer's instruction.

The hypoxia and monocrotaline induced PAH rat models

Two experimental PAH models induced by chronic hypoxia and monocrotaline (MCT) were employed. Chronic hypoxia rats were exposed to 10% O2 in the normorbaric chamber and MCT rats were injected subcutaneously in a hind limb with MCT (60 mg/kg, Sigma). The lungs were collected from control, 2 days, 1 week, 2 weeks hypoxia rats (n=3-4) and 1 week, 2 weeks, 3 weeks and 4 weeks after MCT (n=3-4) injection and stored at -80ºC.

Statistics

The data were expressed as mean $\pm$ SD and analyzed using the student's T-test. One way analysis of variance (ANOVA) followed by Turkey's post hoc tests were carried out for comparison of multiple means. A p-value of ≤ 0.05 indicated statistical significance.

Acknowledgements

The TAK1 plasmid and mouse PASMCs were generous gifts from Dr. H.M. Arthur (Newcastle) and Prof. N.W. Morrell (Cambridge), respectively. This work was supported by a fellowship (awarded to MTN) from the Department of Health via the NIHR Comprehensive Biomedical Research Centre award to Guy's & St Thomas' NHS Foundation Trust in partnership with King's College London. The authors acknowledge financial support from the British Heart Foundation, UK (programme grant 1-2004-357 to RCT) and Heptagon Life Science Proof of Concept Fund (grants KCL24 and KCL25 to MTN and RCT, respectively).

Conflict of interest statement

None.

References

1 Lane, K.B., Machado, R.D., Pauciulo, M.W., Thomson, J.R., Phillips, J.A., 3rd, Loyd, J.E., Nichols, W.C. and Trembath, R.C. (2000) Heterozygous germline mutations in BMPR2, encoding a TGF-beta receptor, cause familial primary pulmonary hypertension. The International PPH Consortium. *Nat Genet*, **26**, 81-84.

2 Atkinson, C., Stewart, S., Imamura, T., Trembath, R.C. and Morrell, N.W. (2001) Immunolocalisation of BMPR-II and TGF-ss type I and II receptors in primary plexogenic pulmonary hypertension. *J Heart Lung Transplant*, **20**, 149.

3 Dewachter, L., Adnot, S., Guignabert, C., Tu, L., Marcos, E., Fadel, E., Humbert, M., Dartevelle, P., Simonneau, G., Naeije, R. *et al.* (2009) Bone morphogenetic protein signalling in heritable versus idiopathic pulmonary hypertension. *Eur Respir J*, **34**, 1100-1110.
4 Dorai, H., Vukicevic, S. and Sampath, T.K. (2000) Bone morphogenetic protein-7 (osteogenic protein-1) inhibits smooth muscle cell proliferation and stimulates the expression of markers that are characteristic of SMC phenotype in vitro. *J Cell Physiol*, **184**, 37-45.
5 Nakaoka, T., Gonda, K., Ogita, T., Otawara-Hamamoto, Y., Okabe, F., Kira, Y., Harii, K., Miyazono, K., Takuwa, Y. and Fujita, T. (1997) Inhibition of rat vascular smooth muscle proliferation in vitro and in vivo by bone morphogenetic protein-2. *J Clin Invest*, **100**, 2824-2832.
6 Yang, X., Long, L., Southwood, M., Rudarakanchana, N., Upton, P.D., Jeffery, T.K., Atkinson, C., Chen, H., Trembath, R.C. and Morrell, N.W. (2005) Dysfunctional Smad signaling contributes to abnormal smooth muscle cell proliferation in familial pulmonary arterial hypertension. *Circ Res*, **96**, 1053-1063.
7 Morrell, N.W., Yang, X., Upton, P.D., Jourdan, K.B., Morgan, N., Sheares, K.K. and Trembath, R.C. (2001) Altered growth responses of pulmonary artery smooth muscle cells from patients with primary pulmonary hypertension to transforming growth factor-beta(1) and bone morphogenetic proteins. *Circulation*, **104**, 790-795.
8 Zhang, S., Fantozzi, I., Tigno, D.D., Yi, E.S., Platoshyn, O., Thistlethwaite, P.A., Kriett, J.M., Yung, G., Rubin, L.J. and Yuan, J.X. (2003) Bone morphogenetic proteins induce apoptosis in human pulmonary vascular smooth muscle cells. *Am J Physiol Lung Cell Mol Physiol*, **285**, L740-754.
9 Thomas, M., Docx, C., Holmes, A.M., Beach, S., Duggan, N., England, K., Leblanc, C., Lebret, C., Schindler, F., Raza, F. *et al.* (2009) Activin-like kinase 5 (ALK5) mediates abnormal proliferation of vascular smooth muscle cells from patients with familial pulmonary arterial hypertension and is involved in the progression of experimental pulmonary arterial hypertension induced by monocrotaline. *Am J Pathol*, **174**, 380-389.
10 Long, L., Crosby, A., Yang, X., Southwood, M., Upton, P.D., Kim, D.K. and Morrell, N.W. (2009) Altered bone morphogenetic protein and transforming growth factor-beta signaling in rat models of pulmonary hypertension: potential for activin receptor-like kinase-5 inhibition in prevention and progression of disease. *Circulation*, **119**, 566-576.
11 Runo, J.R. and Loyd, J.E. (2003) Primary pulmonary hypertension. *Lancet*, **361**, 1533-1544.
12 Welsh, D.J., Peacock, A.J., MacLean, M. and Harnett, M. (2001) Chronic hypoxia induces constitutive p38 mitogen-activated protein kinase activity that correlates with enhanced cellular proliferation in fibroblasts from rat pulmonary but not systemic arteries. *Am J Respir Crit Care Med*, **164**, 282-289.
13 Zeng, Z., Li, Y., Jiang, Z., Wang, C., Li, B. and Jiang, W. The extracellular signal-regulated kinase is involved in the effects of sildenafil on pulmonary vascular remodeling. *Cardiovasc Ther*, **28**, 23-29.
14 Long, L., MacLean, M.R., Jeffery, T.K., Morecroft, I., Yang, X., Rudarakanchana, N., Southwood, M., James, V., Trembath, R.C. and Morrell, N.W. (2006) Serotonin increases susceptibility to pulmonary hypertension in BMPR2-deficient mice. *Circ Res*, **98**, 818-827.
15 West, J., Harral, J., Lane, K., Deng, Y., Ickes, B., Crona, D., Albu, S., Stewart, D. and Fagan, K. (2008) Mice expressing BMPR2R899X transgene in smooth muscle develop pulmonary vascular lesions. *Am J Physiol Lung Cell Mol Physiol*, **295**, L744-755.
16 Weerackody, R.P., Welsh, D.J., Wadsworth, R.M. and Peacock, A.J. (2009) Inhibition of p38 MAPK reverses hypoxia-induced pulmonary artery endothelial dysfunction. *Am J Physiol Heart Circ Physiol*, **296**, H1312-1320.

17 Erdogan, M., Pozzi, A., Bhowmick, N., Moses, H.L. and Zent, R. (2008) Transforming growth factor-beta (TGF-beta) and TGF-beta-associated kinase 1 are required for R-Ras-mediated transformation of mammary epithelial cells. *Cancer Res*, **68**, 6224-6231.
18 Sui, X., Li, D., Qiu, H., Gaussin, V. and Depre, C. (2009) Activation of the bone morphogenetic protein receptor by H11kinase/Hsp22 promotes cardiac cell growth and survival. *Circ Res*, **104**, 887-895.
19 Ishida, W., Hamamoto, T., Kusanagi, K., Yagi, K., Kawabata, M., Takehara, K., Sampath, T.K., Kato, M. and Miyazono, K. (2000) Smad6 is a Smad1/5-induced smad inhibitor. Characterization of bone morphogenetic protein-responsive element in the mouse Smad6 promoter. *J Biol Chem*, **275**, 6075-6079.
20 Watkins, S.J., Jonker, L. and Arthur, H.M. (2006) A direct interaction between TGFbeta activated kinase 1 and the TGFbeta type II receptor: implications for TGFbeta signalling and cardiac hypertrophy. *Cardiovasc Res*, **69**, 432-439.
21 Nasim, M.T., Ghouri, A., Patel, B., James, V., Rudarakanchana, N., Morrell, N.W. and Trembath, R.C. (2008) Stoichiometric imbalance in the receptor complex contributes to dysfunctional BMPR-II mediated signalling in pulmonary arterial hypertension. *Hum Mol Genet*, **17**, 1683-1694.
22 Shim, J.H., Greenblatt, M.B., Xie, M., Schneider, M.D., Zou, W., Zhai, B., Gygi, S. and Glimcher, L.H. (2009) TAK1 is an essential regulator of BMP signalling in cartilage. *Embo J*, **28**, 2028-2041.
23 Hoffmann, A., Preobrazhenska, O., Wodarczyk, C., Medler, Y., Winkel, A., Shahab, S., Huylebroeck, D., Gross, G. and Verschueren, K. (2005) Transforming growth factor-beta-activated kinase-1 (TAK1), a MAP3K, interacts with Smad proteins and interferes with osteogenesis in murine mesenchymal progenitors. *J Biol Chem*, **280**, 27271-27283.
24 Edlund, S., Bu, S., Schuster, N., Aspenstrom, P., Heuchel, R., Heldin, N.E., ten Dijke, P., Heldin, C.H. and Landstrom, M. (2003) Transforming growth factor-beta1 (TGF-beta)-induced apoptosis of prostate cancer cells involves Smad7-dependent activation of p38 by TGF-beta-activated kinase 1 and mitogen-activated protein kinase kinase 3. *Mol Biol Cell*, **14**, 529-544.
25 Soon, E., Holmes, A.M., Treacy, C.M., Doughty, N.J., Southgate, L., Machado, R.D., Trembath, R.C., Jennings, S., Barker, L., Nicklin, P. *et al.* Elevated levels of inflammatory cytokines predict survival in idiopathic and familial pulmonary arterial hypertension. *Circulation*, **122**, 920-927.
26 Steiner, M.K., Syrkina, O.L., Kolliputi, N., Mark, E.J., Hales, C.A. and Waxman, A.B. (2009) Interleukin-6 overexpression induces pulmonary hypertension. *Circ Res*, **104**, 236-244, 228p following 244.
27 Blanco, S., Santos, C. and Lazo, P.A. (2007) Vaccinia-related kinase 2 modulates the stress response to hypoxia mediated by TAK1. *Mol Cell Biol*, **27**, 7273-7283.
28 Matsumoto-Ida, M., Takimoto, Y., Aoyama, T., Akao, M., Takeda, T. and Kita, T. (2006) Activation of TGF-beta1-TAK1-p38 MAPK pathway in spared cardiomyocytes is involved in left ventricular remodeling after myocardial infarction in rats. *Am J Physiol Heart Circ Physiol*, **290**, H709-715.
29 Koitabashi, N., Danner, T., Zaiman, A.L., Pinto, Y.M., Rowell, J., Mankowski, J., Zhang, D., Nakamura, T., Takimoto, E. and Kass, D.A. Pivotal role of cardiomyocyte TGF-beta signaling in the murine pathological response to sustained pressure overload. *J Clin Invest*, **121**, 2301-2312.
30 Melisi, D., Xia, Q., Abbruzzese, J.L. and Chiao, P.J. (2009) TGF-ß-activated kinase 1 (TAK1) is an in vivo druggable target for reverting pancreatic cancer chemoresistance
European Journal of Cancer Supplements
7, 87.

31 Nasim, M.T., Chernova, T.K., Chowdhury, H.M., Yue, B.G. and Eperon, I.C. (2003) HnRNP G and Tra2beta: opposite effects on splicing matched by antagonism in RNA binding. *Hum Mol Genet*, **12**, 1337-1348.
32 Nasim, M.T. and Eperon, I.C. (2006) A double-reporter splicing assay for determining splicing efficiency in mammalian cells. *Nature Protocols*, **1**, 1022-1028.
33 Nasim, M.T. and Trembath, R.C. (2005) A dual-light reporter system to determine the efficiency of protein-protein interactions in mammalian cells. *Nucleic Acids Res*, **33**, e66.

Figure Legends

Figure 1

Dysregulated BMPR-II signaling exerts pro-proliferative activity through the activation of TGFβ signaling. (A) *PAI*-1 expression in mouse primary PASMCs derived from wild-type (*bmpr2*$^{+/+}$) and mutant (*bmpr2* $^{R899X+/-}$) mice and (B) hypoxic rat lung. (C) The effect of TGFβ1 induced p38-MAPK signaling on PASMC proliferation. The relative proliferation rate of wild-type cells was set as 100. (D) Anti- and pro-proliferative responses to TGFβ1 in wild-type and mutant cells. The proliferation rate of both unstimulated wild-type and mutant cells was set as 100. (E) Phosphorylation (Thr180/Thr182) of p38MAPK in PASMCs. TGFβ1 stimulation is indicated by (+). (F) Quantification of p38MAPK phosphorylation derived from three independent western blot analyses. *P<0.05, **P<0.01 and ***P<0.001 compared with normoxic, wild-type or cells stimulated with TGFβ1.

Figure 2

Inhibition of abnormal cell proliferation by selective small molecule inhibitors of TAK1-MAPK pathways in mouse primary PASMCs. (A) The relative level of proliferation of mutant PASMCs compared to wild-type in the presence of 10μM of SD208 and SB203580. (B) As in (A), following stimulation with TGFβ1. (C) The dose-dependent effect of oxozeaenol on the proliferation of wild-type and mutant PASMCs. (D) The inhibitory effect of SB203580 and oxozeaenol on mutant PASMCs. The concentration of TGFβ was 10 ng/ml and the concentration of the inhibitors used was as indicated. Black and grey bars represent

wild-type and mutant cells, respectively. The relative proliferation rate of both wild-type and mutant cells was set at 100. Data are presented as the mean ± SD from 3–6 independent experiments. *P<0.05, **P<0.01 and ***P<0.001 compared with wild-type, mutant or cells stimulated with TGFβ1.

Figure 3

Activation of apoptosis by small molecule drugs that target the TAK1-MAPK pathways. Relative caspase 3/7 activity of (A) wild-type and mutant PASMCs (B) in the presence and absence of staurosporine (ST) or (C) in the presence of SD208 and SB203580. (D) As in (C), following stimulation with TGFβ1. (E) The effect of oxozeaenol on caspase activity in wild-type and mutant PASMCs. (F) The effect of SB203580 and oxozeaenol on caspase 3/7 activity in mutant PASMCs following TGFβ1 stimulation. The relative caspase activity of untreated cells was set at 100. Data are presented as the mean ± SD from 3 independent experiments. The relative caspase activity of both wild-type and mutant cells was set at 100. *P<0.05, **P<0.01 and ***P<0.001 compared with wild-type, mutant or cells stimulated with TGFβ1.

Figure 4

Activation of the TAK1 pathway in hypoxic and monocrotaline-induced PAH rat lung tissue. (A) The relative level of *TAK*1 transcript in normoxic control and hypoxic rat lung. (B) Western blot using phospho-TAK1 (Thr184/187) antibody in a time course of hypoxic rat lungs and (C) quantification of phospho-TAK1 western blots relative to β-actin. (D) Phosphorylation of TAK1 following 1 week of monocrotaline treatment (MCT) and (E) quantification of phospho-TAK1 western blot images. (F-G) Elevated levels of ERK1/2 phosphorylation in rat lungs following 3 weeks of monocrotaline treatment as demonstrated by immunoblotting. *P<0.05 and **P<0.01 compared with control.

Figure 5

Inhibition of BMP signaling by TAK1. (A) The effect of TAK1 on BMP signaling measured with the 3GC2-Lux reporter (19) in the presence of plasmids encoding BMPR-II, ALK3, ALK6, and TAK1. (B) The efficiency of TAK1-mediated inhibition of the reporter. (C) Competition between TAK1 and SMAD1. Concentration of the TAK1 plasmid was 0.25 ng while the SMAD1 plasmid was transfected at 1:1, 1:10, 1:100 and 1:1000, as indicated. The presence and absence of the TAK1 and SMAD1 plasmids are indicated by (+) and (-), respectively. (D) The effect of oxozeaenol treatment on TAK1-mediated inhibition of reporter activity. Data are presented as the mean ± SD from 3–6 independent experiments. *P<0.05, **P<0.01 and ***P<0.001 compared to the reporter.

Figure 6

Interaction of TAK1 and BMPR-II determined by mammalian two hybrid protein-protein interaction assay (33). (A) Dual-light reporter assay. In the event of no interaction, the reporter generates only DsRed-Express protein. Interaction produces both DsRed-Express and GFP. (B) Fluorescence microscopy of HEK293T cells transfected with plasmids encoding BMPR-II fused to the activation domain (BMPRII-AD) and TAK1 fused to the DNA binding domain (TAK1-DBD) compared to reporter alone (TN126). (C) Enzyme based reporter assay. DsRed-Express and GFP genes are replaced by genes encoding β-galactosidase and luciferase (33). (D) Fold activation in HEK293T cells transfected with the enzyme-based reporter, BMPR-II-AD, or TAK1-DBD plasmids. (E) The efficiency of the interaction of BMPR-II with ALK3 and TAK1. The efficiency of the interaction between BMPR-II and TAK1 was set as 1. (F) The relative luc-gal ratio in cells overexpressing mutant BMPR-II and TAK1 compared to the wild-type BMPR-II receptor. Data are presented as mean ± SD from 3–6 independent experiments. Pr- promoter, D/A unit-

deactivation/activation unit for downstream transcription (33). ***P<0.001 compared with reporter or reporter transfected with BMPR-II-AD and TAK1-DBD plasmids. AD indicates activation domain; DBD, DNA-binding domain.

Figure 7

Model depicting the regulation of TGFβ-induced SMAD-independent MAPK pathways in healthy individuals (A) and PAH subjects harbouring a mutation in the *BMPR2* gene (B). (A) BMPR-II–mediated signaling controls the SMAD1/5/8 pathway, and regulates proliferation and apoptosis. In the presence of fully functional BMPR-II–mediated signaling (heavier arrows), the MAPK-mediated anti-apoptotic and pro-proliferative activity of TGFβ signaling is restricted (thinner arrows). The arrows from the central TAK1 pool denote the availability of TAK1 for both the BMP and TGFβ pathways. In BMP signaling, TAK1 is retained by the BMPR-II receptor complex. (B) BMPR-II dysfunction may alter the ratio of cell apoptosis to proliferation and thereby mediating pulmonary vascular hypertrophy. Mutation in *BMPR2* impairs SMAD1/5/8 signaling and makes TAK1 accessible to the TGFβ receptor complex, leading to abnormal proliferation and apoptosis (heavier arrows). Selected inhibition of the TGFβ-mediated TAK1-MAPK pathways by chemical agents is indicated.

Supplementary Figure 1

A

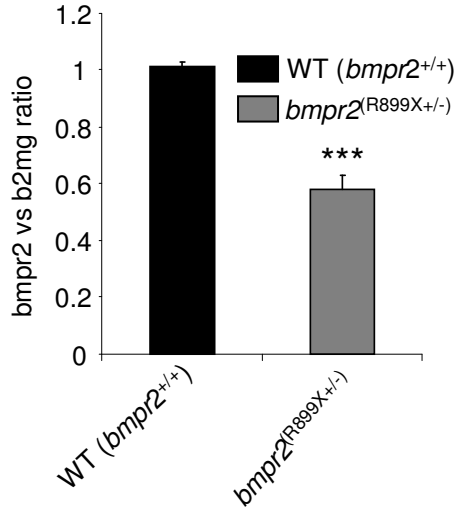

B

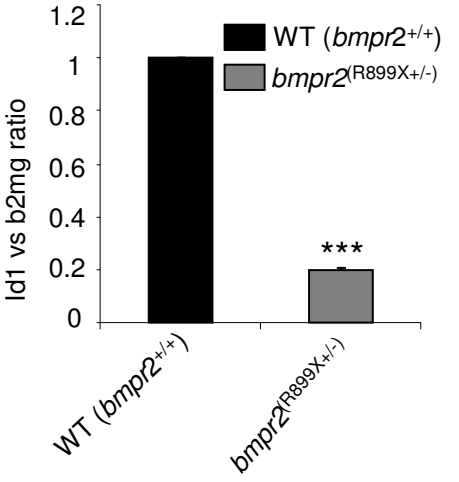

C

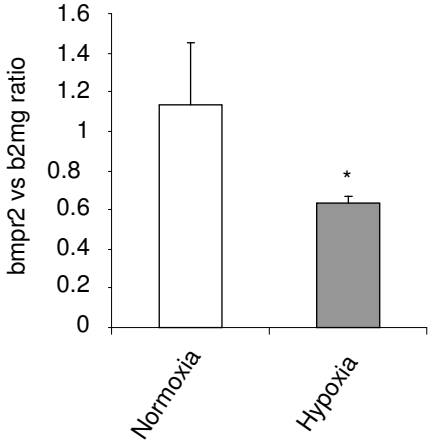

Supplementary Figure 2

A

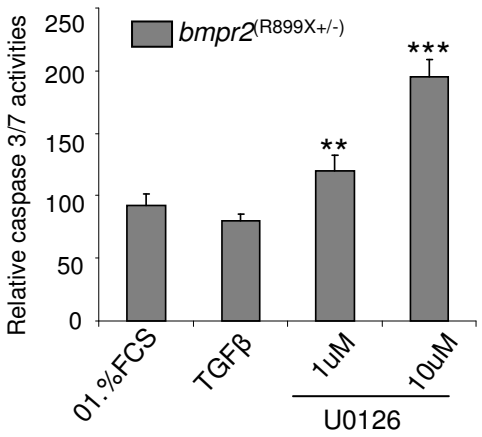

B

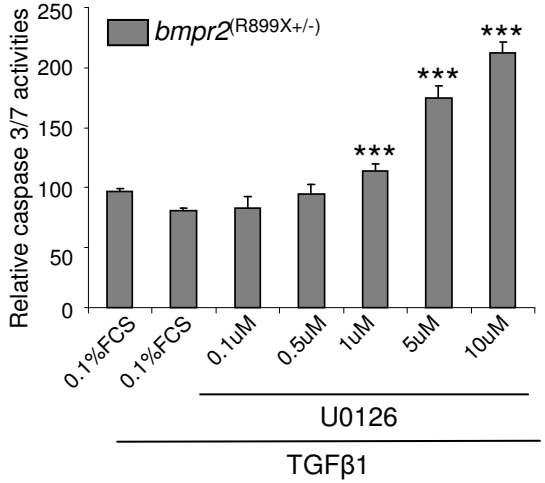

Supplementary Figure 3

A

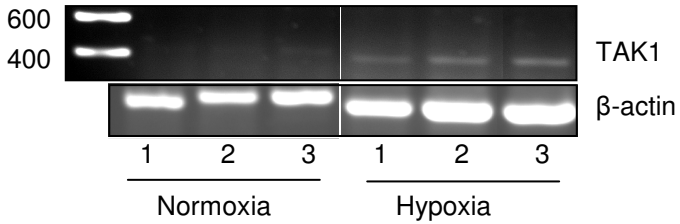

B

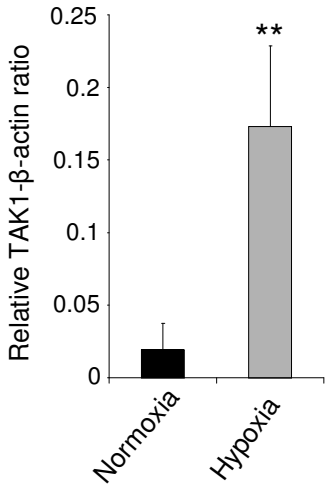

C

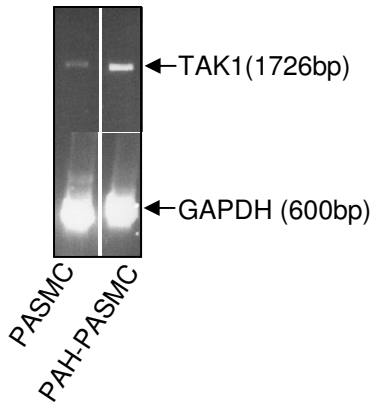

Supplementary Figure 4

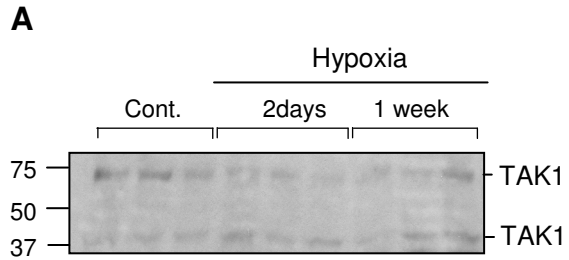

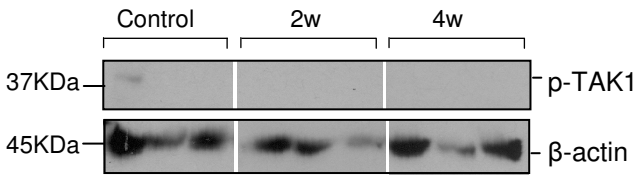

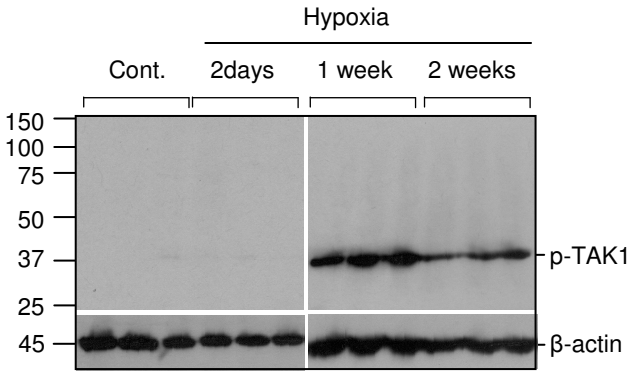

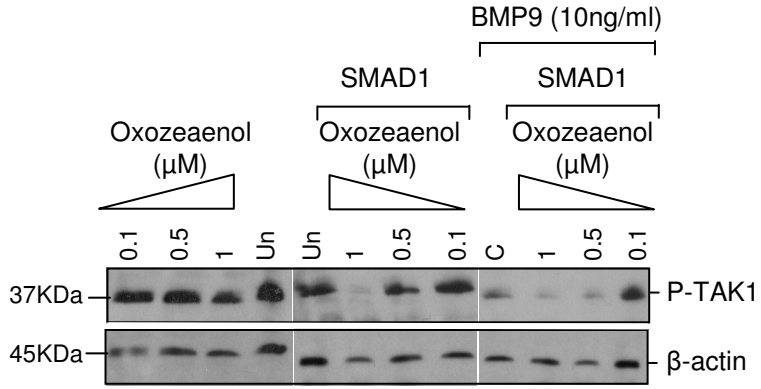

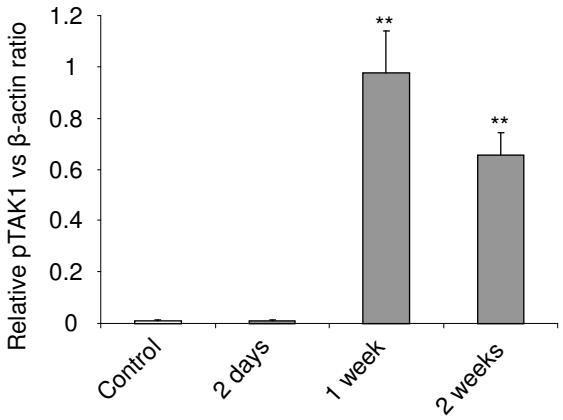

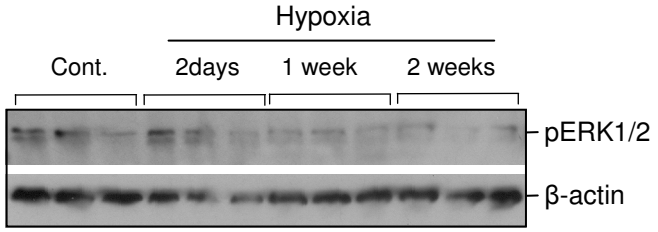

A

Supplementary Figure 5

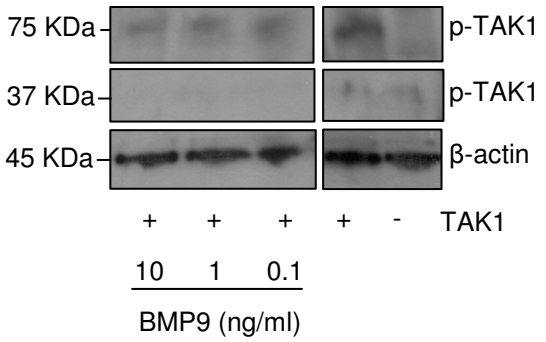

B

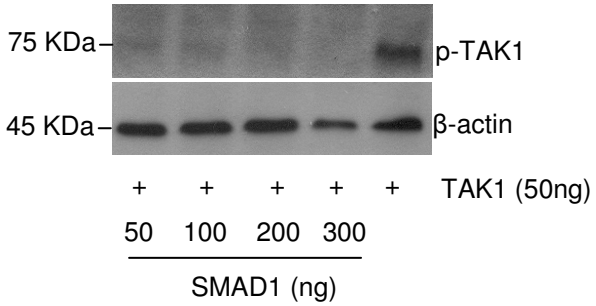

C

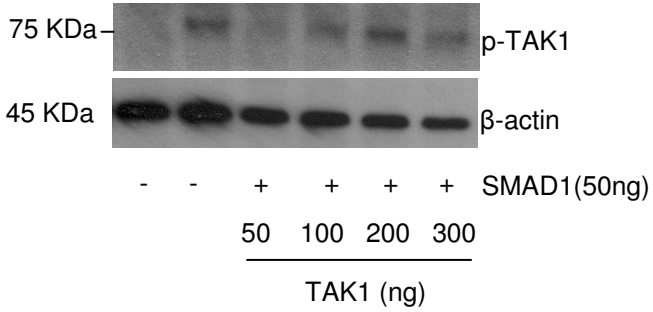

Supplementary Figure 6

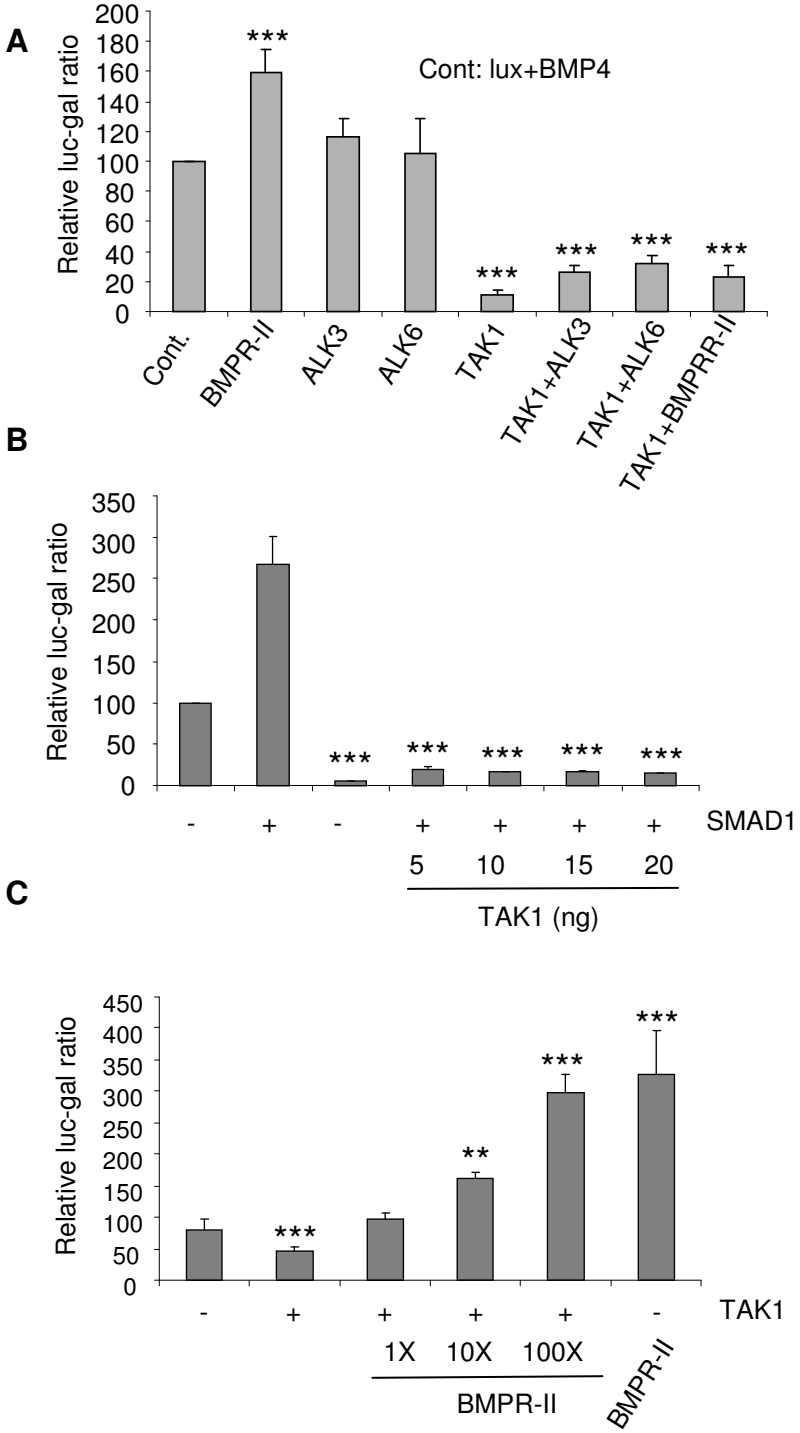

Supplementary Figure 7

A

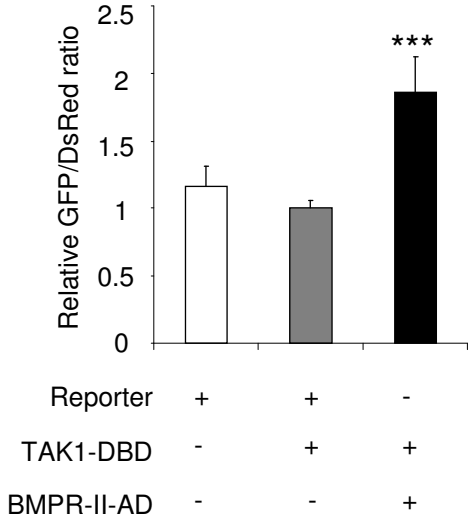

B

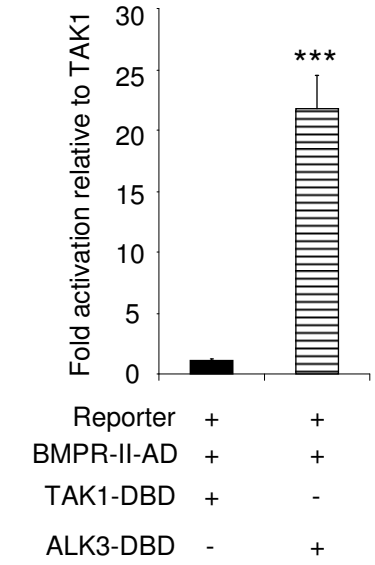

Figure 1

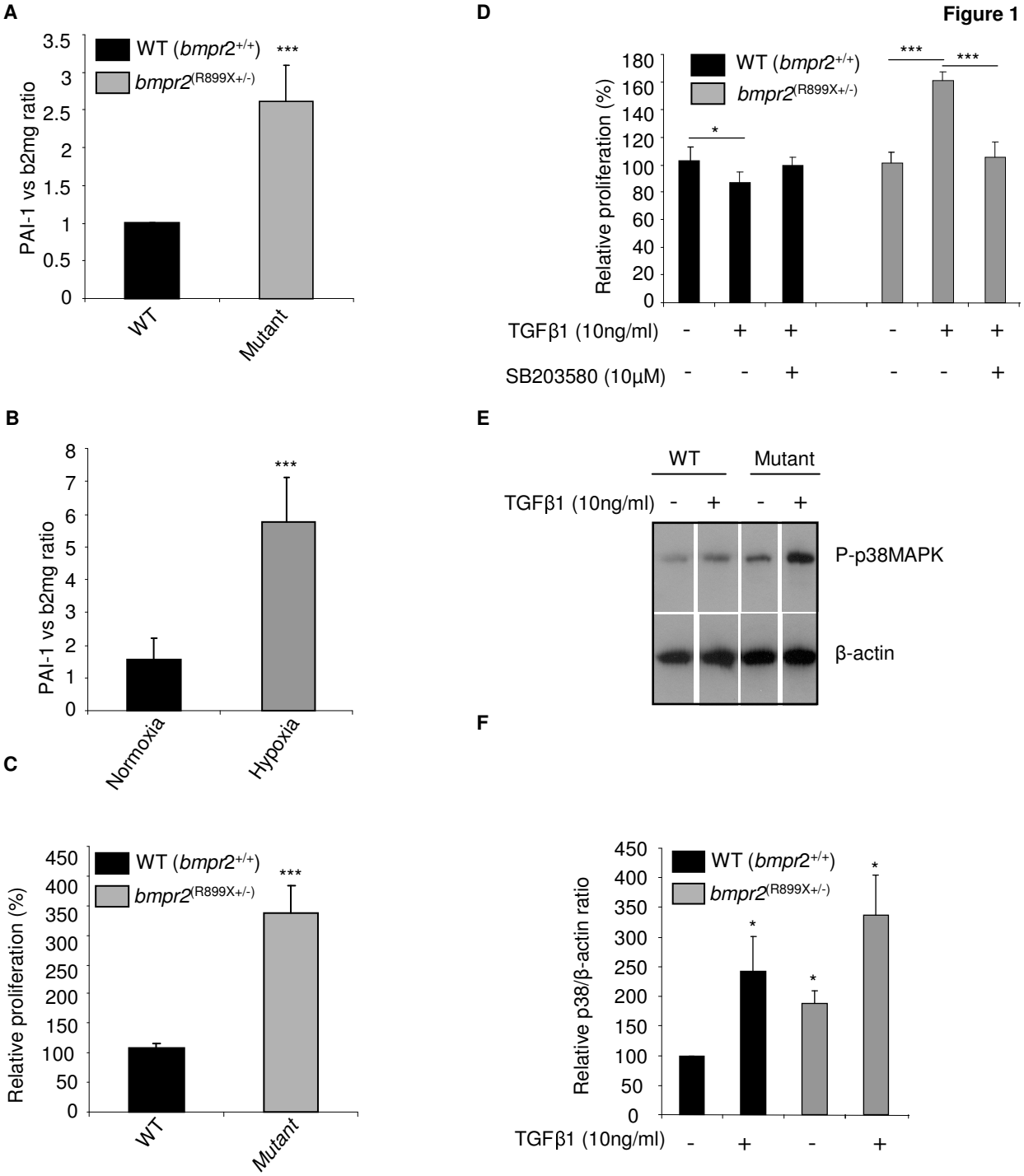
A
WT (bmpr2+/+)
bmpr2(R899X+/-)
PAI-1 vs b2mg ratio
WT
Mutant
B
PAI-1 vs b2mg ratio
Normoxia
Hypoxia
C
Relative proliferation (%)
WT
Mutant
D
Relative proliferation (%)
TGFβ1 (10ng/ml)
SB203580 (10μM)
E
WT
Mutant
TGFβ1 (10ng/ml)
P-p38MAPK
β-actin
F
Relative p38/β-actin ratio
TGFβ1 (10ng/ml)

Figure 2

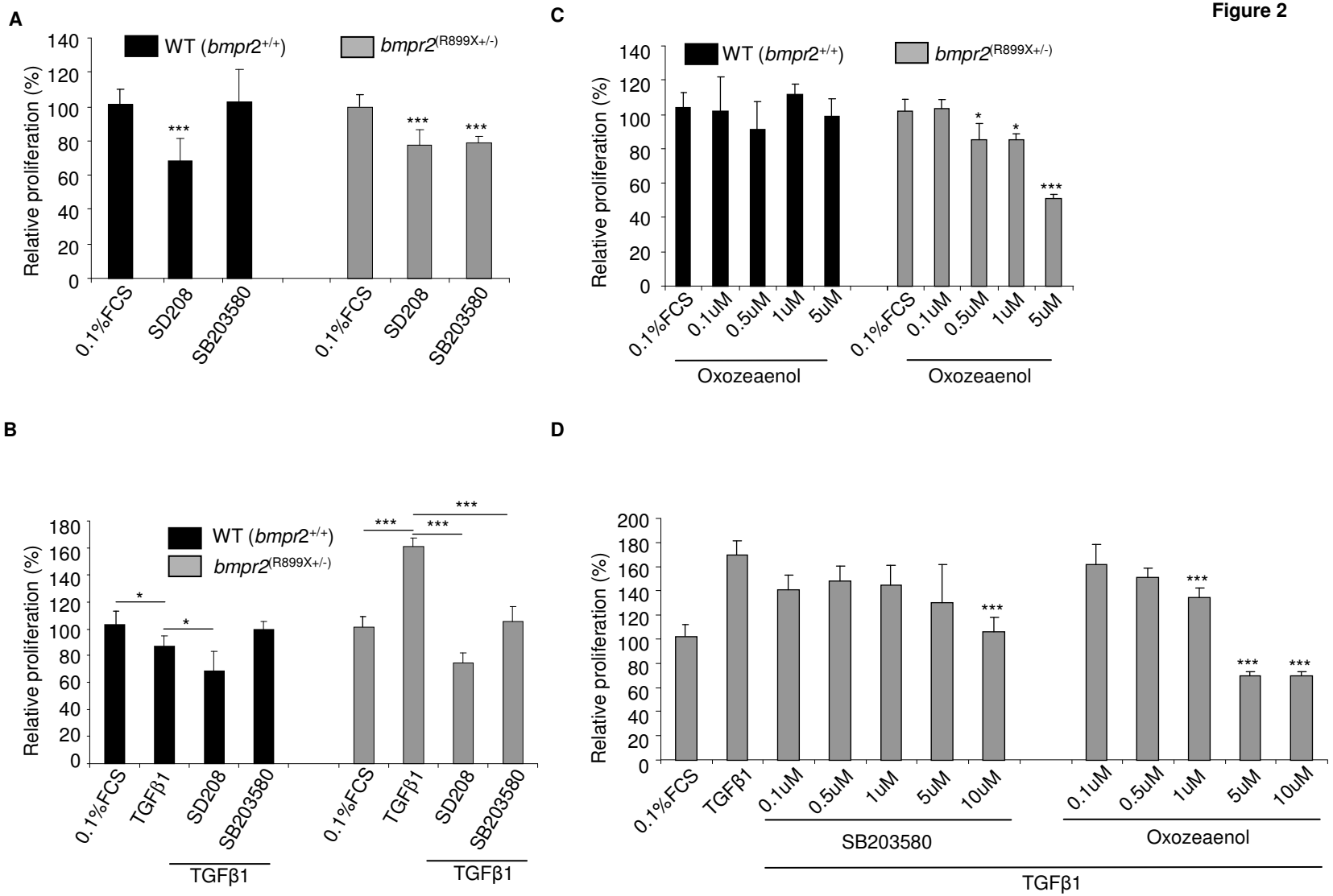
A
WT (bmpr2+/+)
bmpr2(R899X+/-)
Relative proliferation (%)
0.1%FCS
SD208
SB203580
C
Oxozeaenol
B
TGFβ1
D
SB203580
Oxozeaenol

Figure 3

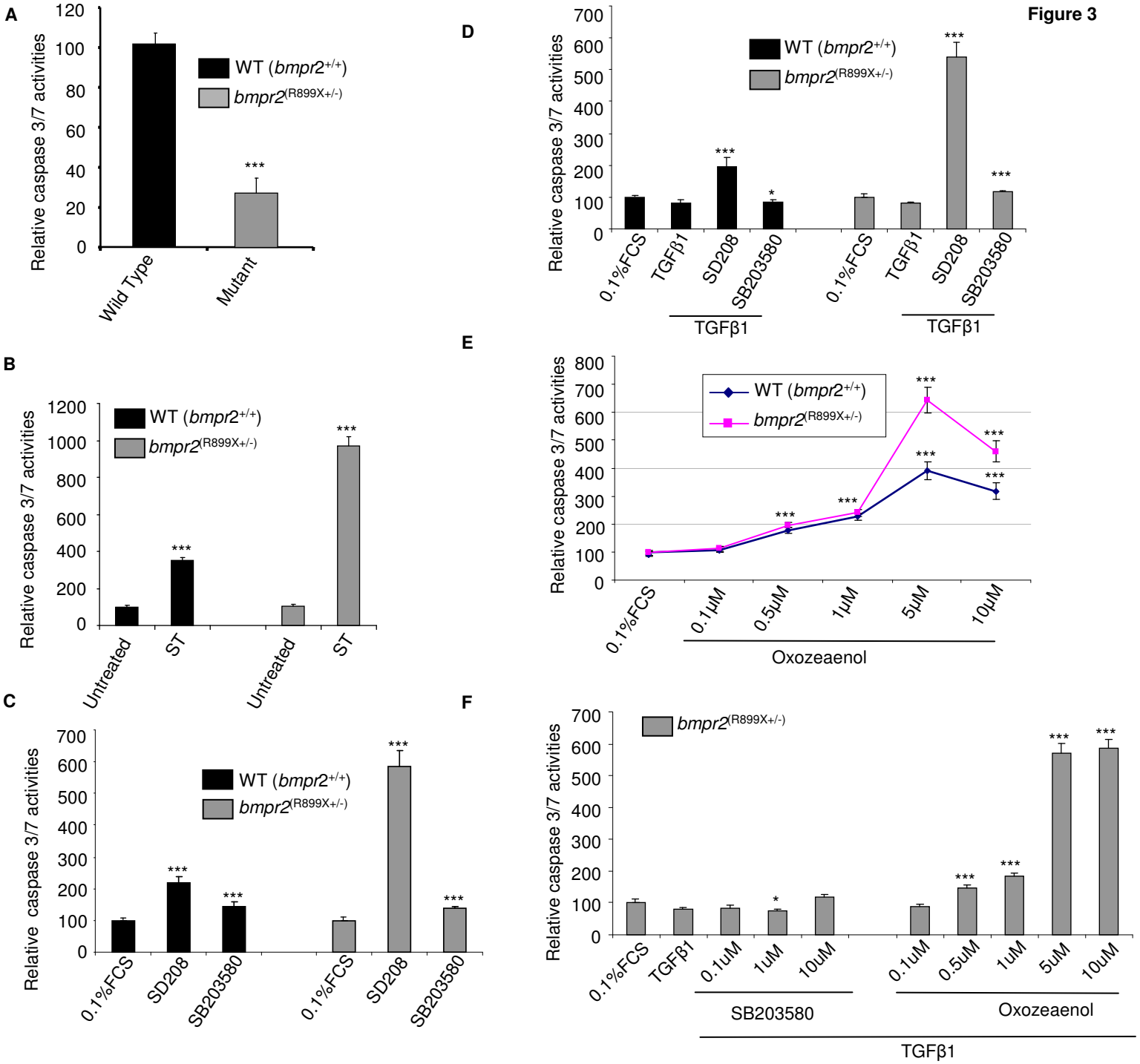
A
Relative caspase 3/7 activities
WT (bmpr2+/+)
bmpr2(R899X+/-)
Wild Type
Mutant
B
Relative caspase 3/7 activities
WT (bmpr2+/+)
bmpr2(R899X+/-)
Untreated
ST
C
Relative caspase 3/7 activities
WT (bmpr2+/+)
bmpr2(R899X+/-)
0.1%FCS
SD208
SB203580
D
Relative caspase 3/7 activities
WT (bmpr2+/+)
bmpr2(R899X+/-)
0.1%FCS
TGFβ1
SD208
SB203580
E
Relative caspase 3/7 activities
WT (bmpr2+/+)
bmpr2(R899X+/-)
0.1%FCS
0.1μM
0.5μM
1μM
5μM
10μM
Oxozeaenol
F
Relative caspase 3/7 activities
bmpr2(R899X+/-)
0.1%FCS
TGFβ1
0.1uM
1uM
10uM
0.5uM
5uM
SB203580
Oxozeaenol
TGFβ1

Figure 4

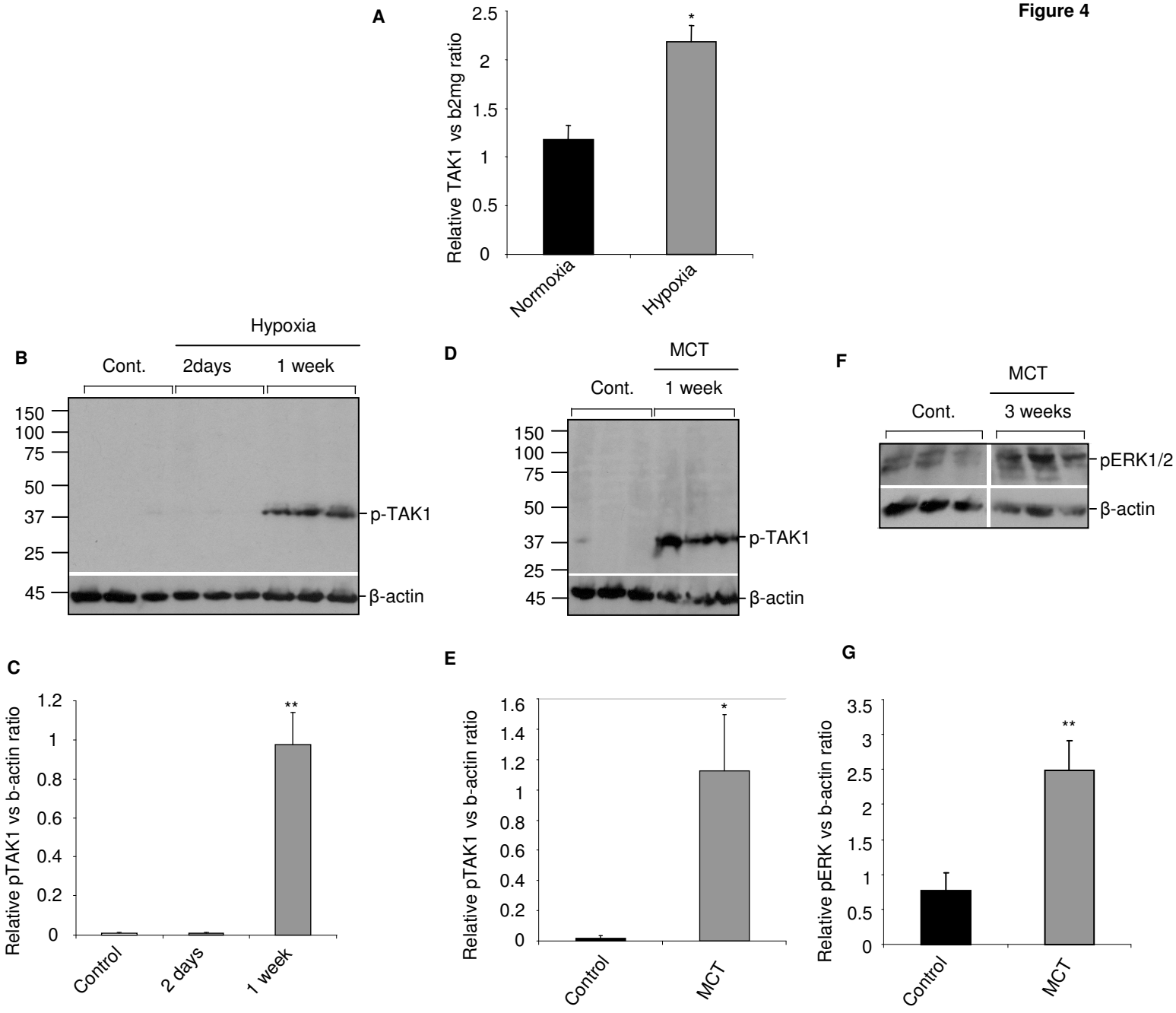
A
Relative TAK1 vs b2mg ratio
2.5
2
1.5
1
0.5
0
*
Normoxia
Hypoxia
B
Hypoxia
Cont.
2days
1 week
150
100
75
50
37
25
45
p-TAK1
β-actin
D
MCT
Cont.
1 week
150
100
75
50
37
25
45
p-TAK1
β-actin
F
MCT
Cont.
3 weeks
pERK1/2
β-actin
C
Relative pTAK1 vs b-actin ratio
1.2
1
0.8
0.6
0.4
0.2
0
**
Control
2 days
1 week
E
Relative pTAK1 vs b-actin ratio
1.6
1.4
1.2
1
0.8
0.6
0.4
0.2
0
*
Control
MCT
G
Relative pERK vs b-actin ratio
3.5
3
2.5
2
1.5
1
0.5
0
**
Control
MCT

Figure 5

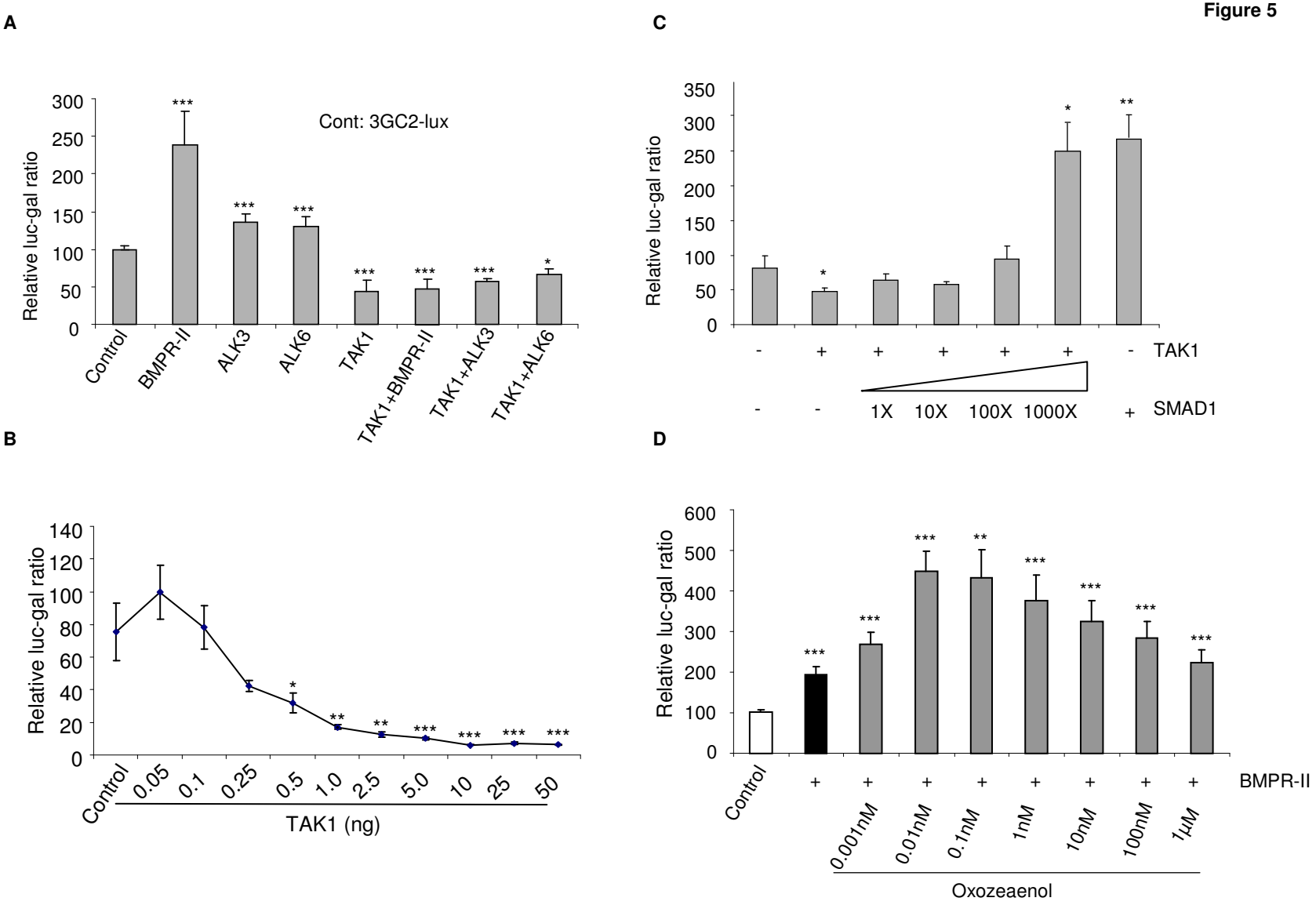
A
Cont: 3GC2-lux
Relative luc-gal ratio
Control
BMPR-II
ALK3
ALK6
TAK1
TAK1+BMPR-II
TAK1+ALK3
TAK1+ALK6
B
Relative luc-gal ratio
Control
0.05
0.1
0.25
0.5
1.0
2.5
5.0
10
25
50
TAK1 (ng)
C
Relative luc-gal ratio
TAK1
SMAD1
1X
10X
100X
1000X
D
Relative luc-gal ratio
Control
BMPR-II
0.001nM
0.01nM
0.1nM
1nM
10nM
100nM
1μM
Oxozeaenol

Figure 6

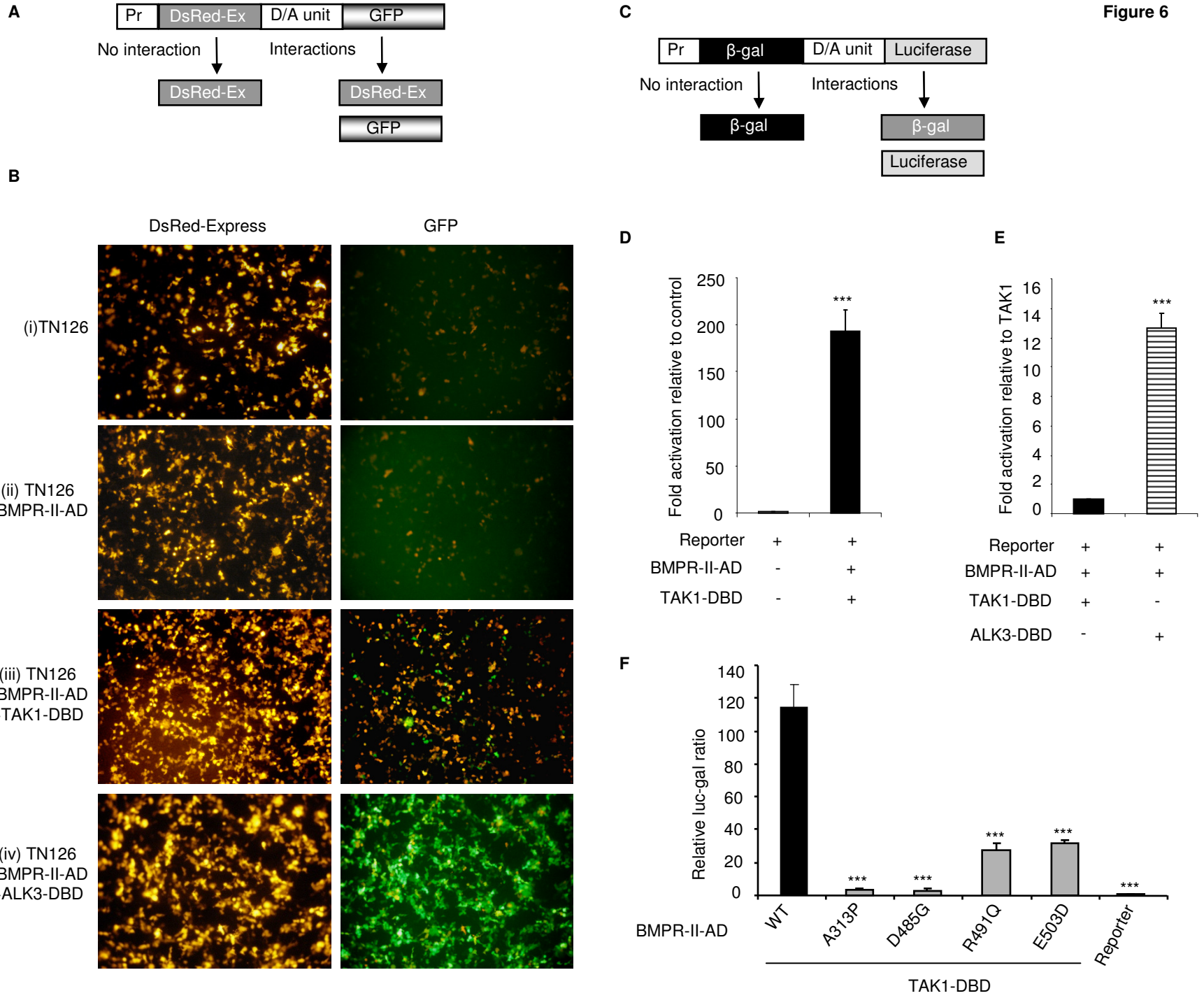
A
Pr
DsRed-Ex
D/A unit
GFP
No interaction
Interactions
DsRed-Ex
DsRed-Ex
GFP
B
DsRed-Express
GFP
(i)TN126
(ii) TN126
+BMPR-II-AD
(iii) TN126
+BMPR-II-AD
+TAK1-DBD
(iv) TN126
+BMPR-II-AD
+ALK3-DBD
C
Pr
β-gal
D/A unit
Luciferase
No interaction
Interactions
β-gal
β-gal
Luciferase
D
Fold activation relative to control
250
200
150
100
50
0
***
Reporter + +
BMPR-II-AD - +
TAK1-DBD - +
E
Fold activation relative to TAK1
16
14
12
10
8
6
4
2
0
***
Reporter + +
BMPR-II-AD + +
TAK1-DBD + -
ALK3-DBD - +
F
Relative luc-gal ratio
140
120
100
80
60
40
20
0
***
***
***
***
***
BMPR-II-AD
WT
A313P
D485G
R491Q
E503D
Reporter
TAK1-DBD

A Normal

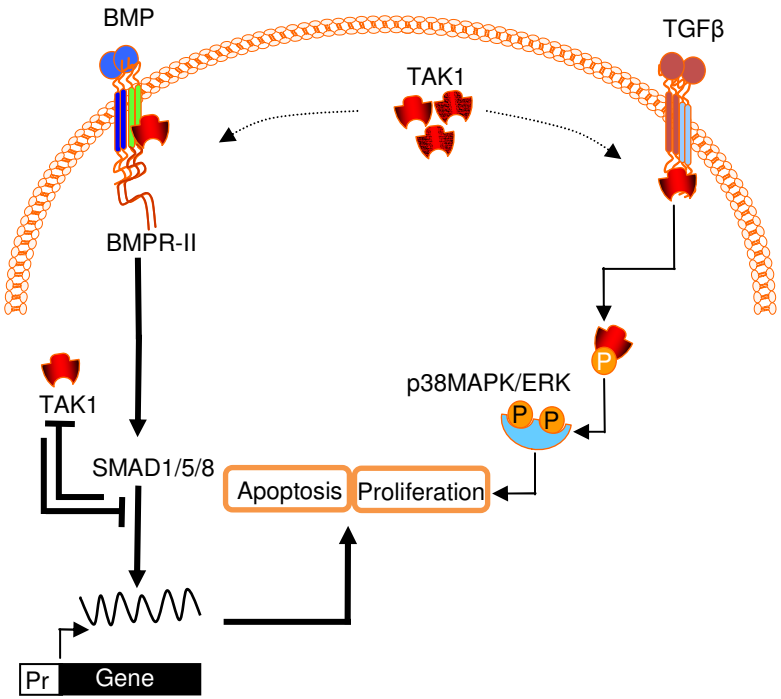

B PAH

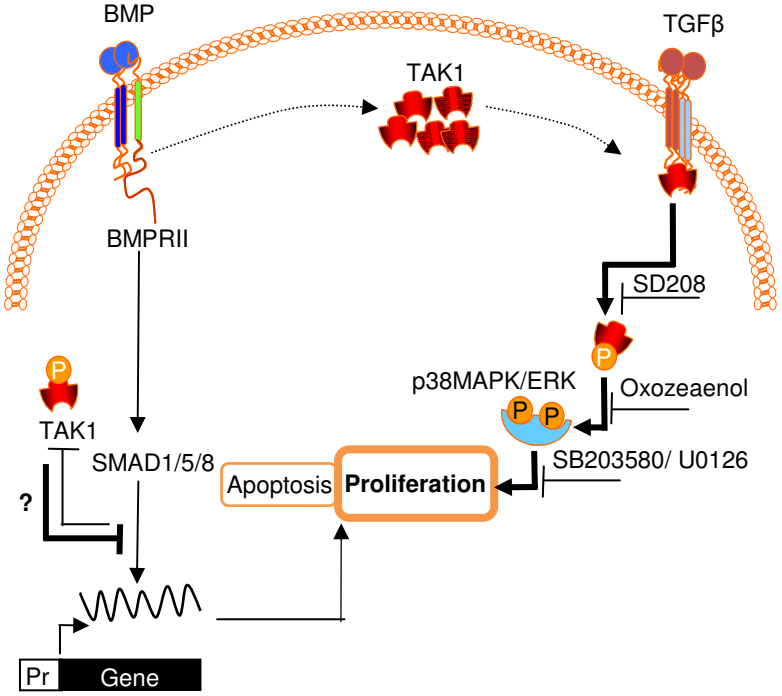

Figure 7

Supplementary data

Materials and Methods

RNA isolation, cDNA synthesis and reverse Transcriptase PCR (RT-PCR)

RNA was isolated from mammalian cells using TRI-Reagent (Sigma), cDNA was synthesized using random primers and MMLV Reverse Transcriptase (Promega) following manufacturer's protocol. Total lung tissue RNA was extracted using the Trizol method (Invitrogen). 2 ug RNA was then reverse transcribed using Thermoscript RT-PCR kits (Invitrogen). The PCR was carried out using Hi-Fidelity Extensor Master Mix (ABgene). Quantitative PCR for determining transcripts of BMPR2, PAI-1, TAK1, Id1 and β-2 microglobulin were performed using TaqMan Gene Expression Assay (Applied Biosystems) on 7900HT Fast Real-Time PCR system (Applied Biosystems) according to the manufacturer's protocol.

Generation of constructs for protein-protein interactions assay

The coding sequence of full-length human TAK1 (accession number BC017715) lacking the first amino acid was cloned into BamHI and XbaI sites of pTN111 vector (1). The resulting plasmid contains a N-terminal DNA binding domain (DBD) adjacent to the human TAK1, the fidelity of which was verified by restriction analyses and sequencing. Efficiency of protein-protein interactions between TAK1 and BMPRII in mammalian cells was determined as previously reported (http://www.natureprotocols.com/2007/06/28/efficiency_of_proteinprotein_i_1.php). In brief the intracellular domain of BMPR-II was fused with VP-16 activation domain (2) whilst TAK1 was fused with a DBD. Plasmids encoding both fusion proteins were transfected into human embryonic kidney (HEK293) cells together with the gal-luc and DsRed-Express-GFP reporters (pTN114 and pTN126; (2)). In the event of an interaction

both reporter proteins will be generated with the ratio of reporter activities producing a measure of the efficiency of protein-protein interactions.

Details of the other expression constructs used in this study are available upon request.

Cell culture, transient transfection, enzymatic and fluorescence assay

Cell culture and transfections were carried out as described elsewhere (2), (3). Luciferase and β-galactosidase activities were determined with the Dual-light Reporter Assay systems (Applied Biosystems) using an ORION-II Plate Luminometer (Berthold) according to manufacturers protocols. BMP-responsive reporter assay in mammalian cells was performed as previously described (2). For determination of fluorescence intensity, cells were grown in 96 well black plate and 24 hours after transfection medium was replaced by DMEM containing 0.1%FBS and grown for an additional 48 hours. At the time of measurement, the medium was discarded and the fluorescence intensities were determined using BMG Labtech Omega fluorescence plate reader.

Quantification of proliferation and apoptosis of mouse primary PASMCs

To determine proliferation, cells were seeded at $0.2X10^{5}$ per well in a clear 96 well plate in DMEM containing 10% FBS. Twenty four hours later, the medium was replaced by either fresh DMEM/0.1% FBS alone or containing TGFβ1 (10ng/ml) (R&D Systems), SD208 (10μM) (TOCRIS), SB203580 (0.1-10 μM) (TOCRIS), (5Z)-7-Oxozeaenol (0.1-10 μM) (TOCRIS) and U0126 (0.1-10 μM) (TOCRIS) and grown for additional for 4-5 days. The relative rate of cell proliferation was determined using CellTiter 96® Aq_{ueous} One Solution Cell Proliferation Assay (Promega) following manufacturer's protocol. Absorbance was recorded at 490nm using Omega Plate Reader (BMG Labtech) at 1, 2 and 3 hours intervals.

For apoptosis assays, cells were seeded as mentioned before with the exceptions that a white 96 well plate was used and assays were carried out 24 hours after the treatment. For induction of apoptosis cells were treated with staurosporine for overnight at

concentrations of 0.2µM. Apoptosis assays were carried out using Caspase-Glo® 3/7 Assay (Promega) following manufacturer's instruction. Luminescence was recorded using ORION-II Plate Luminometer (Berthold).

Western blots analysis

Mouse PASMCs grown in either 6 or 12 well plates were washed with PBS and lysed with 1X Reporter Lysis Buffer (Promega) containing protease and phosphatase inhibitor cocktail (Rochae) together with 1X SDS loading dye in a plate shaker at room temperature for 20 minutes. Cell extracts from HEK293 cells were prepared as above with the exception that cells were undergone a repeated freeze and thaw cycle and without the SDS dye. Cells were centrifuged at 14,000g at 4ºC for 15 minutes. Lung tissues were put (100-200mg) into the Lysing Matrix D tubes (MP Biomedicals), which contain 1ml phosphate buffer (100mM DO4 [K2HPO4:KH2PO4 = 3:1], 1mM EDTA, 1mM DTT) supplemented with protease inhibitor (Roche). Tissues were homogenated by Hybaid Ribolyser **(**Hybaid**).** The protein concentration of the homogenants is determined by BCA protein assay (Thermo scientific).The protein suspension was separated on a (4-20%) SDS-PAGE gel (Bio-Rad), transferred onto a nitrocellulose membrane (Whatmann) and incubated with blocking buffer (1X TBS, 0.1% Tween-20 with 5% w/v nonfat dry milk). Membranes were incubated with phospho-specific p38MAPK (Thr180/Thr182), TAK1 (Thr184/187), ERK1/2 (Thr202/Tyr204) and total TAK1 (Cell signaling) antibodies following manufacturer's protocols. The membrane was developed with an enhanced chemiluminescence reagent (ECL Plus Western blotting Detection Reagents, Amersham). To confirm equal loading the membranes were stripped and re-probed with anti-β-actin antibody (Cell Signaling).

Supplementary Figure Legends

Supplementary Figure 1

Effect of nonsense mutation in the *bmpr2* gene on BMP signaling measured on Id1 gene expression. Determination of the *bmpr2* (A) and *Id1* (B) transcripts relative to β-2-microglobulin (b2mg) in mouse primary PASMCs by quantitative PCR. (C) As in (A), in hypoxic rat lungs. ***P<0.001 compared with wild type PASMCs.

Supplementary Figure 2

The anti-apoptotic phenotype of *bmpr2* mutant PASMCs was rescued by U0126 treatment. Activation of caspase 3/7 activity in the absence (A) and presence of TGFβ stimulation (B). U0126 activates caspase activity in a dose dependent manner. The relative caspase activity of untreated mutant cells (0.1% FCS) was set as 100. *P<0.05, **P<0.01 and ***P<0.001 compared with untreated cells.

Supplementary Figure 3

Increased expression of TAK1 in hypoxic PAH rat lungs and PAH-PASMCs. (A) RT-PCR analysis of TAK1 transcripts in lung samples derived from normoxic and hypoxic rats (n=3). (B) Quantification of RT-PCR by image analysis. (C) RT-PCR of TAK1 transcripts in PAH-PASMCs. The sizes of DNA bands derived from TAK1 and GAPDH transcripts are indicated.

Supplementary Figure 4

Activation of TAK1 in PAH rat lungs. (A) Western blot analysis of total TAK1 proteins in hypoxic rat lungs detecting a long (TAK1-LF) and a short (TAK1-SF) isoform. Transient activation of TAK1-SF in hypoxic PAH rat model (B-C). Data associated with time course 2 days and 1 week were presented in Figure 4B-C and are included here for comparison. (D) TAK1-SF was phosphorylated following 1 week (see Figure 4D) but not in 2 and 4 week of monocrotaline treatment. (E) Oxozeaenol treatment and BMP9 stimulation inhibit the phophorylation of TAK1-SF in HEK293T cells. (F) Western blot using phopho-

ERK1/2 antibody in a time course of hypoxic rat lungs. ***P<0.001 compared with normoxia.

Supplementary Figure 5

Negative regulation of TAK1 by BMP signaling in HEK293 cells. (A) BMP9 inhibits the phosphorylation of endogenousTAK1-SF and overexpressed TAK1. (B) SMAD1 overexpression inhibits the phosphorylation of TAK1 in a dose dependent manner. (C) SMAD1 mediated inhibition of TAK1 phosphoryaltion was rescued by overexpression of TAK1.

Supplementary Figure 6

Inhibition of BMP signalling by TAK1. (A) Effect of TAK1 on BMP signaling measured on the 3GC2-Lux reporter in the presence of plasmids encoding BMPR-II, ALK3, ALK6, and TAK1 in HEK293 cells stimulated with BMP4 ligand. (B) Competition between TAK1 and SMAD1. Concentration of SMAD1 plasmid was 100ng whilst the TAK1 plasmid was transfected at 5, 10, 15 and 20ng as indicated. (C) Effect of BMPR-II overexpression on TAK1–mediated inhibition of reporter activity. Concentration of TAK1 plasmid was 0.25ng whilst the BMPR-II plasmid was transfected at 1:1, 1:10 and 1:100 ratio as indicated. The presence and absence of TAK1, SMAD1 and BMPR-II plasmid were indicated by (+) and (-), respectively. Data are presented as mean ± SD which were derived from 3 independent experiments. **P<0.01 and ***P<0.001 compared with reporter.

Supplementary Figure 7

Interaction of TAK1 and BMPR-II determined by mammalian two hybrid dual-fluorescence protein interactions assay (1). (A) The relative GFP-DsRed-Express ratio in HEK293T cells overexpressing BMPR-II-AD and TAK1-DBD together with the fluorescence reporter (TN126). The ratio was both fluorescence intensities was compared in cells transfected with reporter alone or with TAK-DBD. (B) The efficiency of

interactions of BMPR-II with ALK3 and TAK1 determined by the fluorescence assay. Efficiency of interactions between BMPR-II and TAK1 was set as 1. Data are presented as mean ± SD which were derived from 3 independent experiments. ***P<0.001 compared with reporter.

References

1 Nasim, M.T. and Trembath, R.C. (2005) A dual-light reporter system to determine the efficiency of protein-protein interactions in mammalian cells. *Nucleic Acids Res*, **33**, e66.

2 Nasim, M.T., Ghouri, A., Patel, B., James, V., Rudarakanchana, N., Morrell, N.W. and Trembath, R.C. (2008) Stoichiometric imbalance in the receptor complex contributes to dysfunctional BMPR-II mediated signalling in pulmonary arterial hypertension. *Hum Mol Genet*, **17**, 1683-1694.

3 Nasim, M.T. and Eperon, I.C. (2006) A double-reporter splicing assay for determining splicing efficiency in mammalian cells. *Nature Protocols*, **1**, 1022-1028.